J Mater Sci (2007) 42:7696–7701
DOI 10.1007/s10853-007-1673-z

Synthesis and electrochemical characterization of $LiCo_{1/3}Ni_{1/3}Mn_{1/3}O_2$ by radiated polymer gel method

J. W. Wen · H. J. Liu · H. Wu · C. H. Chen

Received: 10 December 2006 / Accepted: 8 March 2007 / Published online: 3 June 2007

Abstract Layered $LiCo_{1/3}Ni_{1/3}Mn_{1/3}O_2$ as a lithium insertion positive-electrode material was prepared by a radiated polymer gel method. The synthesis conditions and microstructure, morphology and electrochemical properties of the products were investigated by XRD, SEM and electrochemical cell cycling. It was found that the positive-electrode material annealed at 950 °C showed the best electrochemical property with the first specific discharge capacity of 178 mAh/g at C/6 and stable cycling ability between 2.8 and 4.5 V versus Li/Li^+. The optimized $LiCo_{1/3}Ni_{1/3}Mn_{1/3}O_2$ exhibited rather good rate capability with the specific capacity of 173 mAh/g at 0.2C and 116 mAh/g at 4C under a fast charge and discharge mode in rate performance test.

Introduction

Lithium-ion batteries are playing more and more important role in many kinds of electronic devices. Currently, lithium cobalt oxide ($LiCoO_2$) that was initially introduced by Goodenough [1] has been widely used in lithium secondary batteries as a commercial positive-electrode material [1, 2]. The problems of this material lie in its high cost and relative toxicity of cobalt element, and especially the relative thermal instability of $LiCoO_2$. The recent recall from Dell notebook computers highlights the safety issue of this material, suggesting that the search for alternative positive electrode materials is necessary.

In the last few years, the ternary transition-metal oxide system $LiCo_{1/3}Ni_{1/3}Mn_{1/3}O_2$ has been developed into a strong candidate owing to its high specific capacity, lower cost and stable structure in the wide 2.5–4.5 V voltage range [3–13]. Moreover, $LiCo_{1/3}Ni_{1/3}Mn_{1/3}O_2$ exhibits enhanced safety with higher thermal stability compared with its counterpart $LiCoO_2$. Electronic structure studies have shown that the oxidation states of transition-metal ions in this composition are Ni^{2+}, Co^{3+} and Mn^{4+}, respectively [6, 12–15]. During charge/discharge reactions, there may occur $Ni^{2+}/Ni^{3+}/Ni^{4+}$ and Co^{3+}/Co^{4+} alternating [6, 12, 14, 15], resulting in high specific capacity accompanied with enhanced thermal stability.

The synthesis method is very important to the electrochemical behaviors of the positive-electrode material because of the different particle morphologies resulted from different routes. Up to the present, various synthesis methods have been tried for the preparation of $LiCo_{1/3}Ni_{1/3}Mn_{1/3}O_2$, such as solid state reaction [5], carbonate co-precipitation [16], hydroxide co-precipitation [17], water-in-oil emulsion method [18], spray drying and metal acetate decomposition approaches [19].

Gamma-ray radiation has been widely used in many fields such as the sealing of food, antisepsis of medical instruments and production of cable for its high efficiency and low cost. In this paper, γ-ray radiation has been initially introduced to the process of preparing pure-phase $LiCo_{1/3}Ni_{1/3}Mn_{1/3}O_2$ with a method called radiated polymer gel method (RPG), which was used to synthesize pure phase of $LiCoO_2$ [20] and $LiNi_{0.5}Mn_{1.5}O_4$ [21] previously. RPG is one of sol–gel methods but different from the typical sol–gel method. In this method, γ-radiation is applied to swift formation of homogeneous gel instead of

J. W. Wen · H. J. Liu · H. Wu · C. H. Chen (✉)
Laboratory for Advanced Functional Materials and Devices,
Department of Materials Science and Engineering,
University of Science and Technology of China,
Anhui Hefei 230026, P.R. China
e-mail: cchchen@ustc.edu.cn

the transformation step of sol-to-gel in typical sol-gel method. Since the homogeneous gel polymer can host mixed metal salts, a mixture of metal oxides can be obtained by firing the polymer. Further heat treatment of the mixture may generate lithium metal oxides for positive electrode material of lithium-ion cells. The synthesis conditions particularly the sintering temperature have been optimized to achieve desirable electrochemical properties in this study.

Experimental

A mixture of $LiCH_3COO \cdot 2H_2O$, $Ni(CH_3COO)_2 \cdot 4H_2O$, $Co(CH_3COO)_2 \cdot 4H_2O$ and $Mn(CH_3COO)_2 \cdot 4H_2O$ with a molar ratio of Li:Co:Ni:Mn = 1.05:0.33:0.33:0.33 was dissolved into deionized water to obtain a dark purple aqueous solution. The 5 mol% excess of Li was to compensate for the volatilization of Li during high temperature heating. Then acrylic acid (AA) (CH_2=CHCOOH) was added into the mixture with 1:2(v/v) of AA/water. The pH value of the mixture was controlled around 3.5. Subsequently, Co60 γ-ray radiation (intensity 55–75 Gy/min) was applied on the mixture for 2 h to obtain a dark purple gel, which was caused by the polymerization of the monomer of acrylic acid (AA) on condition of irradiation. The gel was dried in air at 150 °C for 20 h to remove the solvent water. Then it was calcined at 400 °C for 6 h to obtain a powder, which was further annealed at a temperature from 800 to 1,000 °C in air to produce powders with the correct layered structure.

X-ray diffraction patterns of these powders were obtained using an X-ray diffractometer (Philips X'Pert Pro Super, Cu Kα radiation) equipped with a graphite monochromator. A scanning electron microscopy (SEM, HITACHI X-650) study of the powder annealed at 900 and 950 °C was performed to analyze its morphology. Particle size distribution was measured on a laser scattering instrument (Rise-2006).

The electrochemical characterizations were carried out using CR2032-type coin-cells. The positive electrode slurry was fabricated by mixing the $LiCo_{1/3}Ni_{1/3}Mn_{1/3}O_2$, acetylene black and polyvinylidene fluoride with a weight ratio of 84:8:8 in the dispersant agent *N-methly-2-pyrolidinone. This slurry was cast on an aluminum foil to make a positive electrode laminate. The loading of active material on each positive electrode is around 10 mg. Lithium foil was utilized as the negative electrode, and the electrolyte solution was composed of 1.0 M $LiPF_6$ in EC/ DEC (1:1 by volume ratio). The cells were assembled in an argon-filled glove box (MBraun Labmatser 130).*

The cells were charged/discharged between 2.8 and 4.5 V versus Li/Li^+ at room temperature (about 28 °C). The charge/discharge mode of constant current and constant voltage (CCCV) was adopted. During the charge step, the cells were charged at a constant current to 4.5 V, and then kept the voltage at 4.5 V until the current dropped to less than C/20 current. In the first three cycles, the cells were cycled with C/6 rate (180 mAh/g for 1C rate). Then they were cycled at C/2 rate in the following cycles. For the cell using optimized $LiCo_{1/3}Ni_{1/3}Mn_{1/3}O_2$ material, its capacity at various C-rates from 0.2 to 8C was also measured. Cyclic voltammetry (CV) was also performed on a CHI 604B Electrochemical Workstation to determine the characteristics of the lithium reaction with the $LiCo_{1/3}Ni_{1/3}Mn_{1/3}O_2$ positive electrode.

Results and discussion

XRD and SEM analysis

In this preparation method, in order to generate a pure phase of $LiCo_{1/3}Ni_{1/3}Mn_{1/3}O_2$ powder, it is very important to form an immobilized gel with homogeneous mixture of all of the four metal precursors. The gamma-ray can initiate a rapid and homogeneous polymerization of acrylic acid monomers which are associated with metal ions in the precursor solution. In fact, this RPG route easily obtains a translucent gel with only one color. For comparison, we also tried to thermally initiate the polymerization process with the addition of small amount of an initiator (e.g., azobisisobutyronitrile), but the gel obtained was not very homogenous and some impurity phases were found in the final powder product.

Figure 1 shows the X-ray diffraction patterns of $LiCo_{1/3}Ni_{1/3}Mn_{1/3}O_2$ powders that were annealed at different temperatures from 800 to 1,000 °C with a step of 50 °C in air. The XRD patterns of all samples are consistent with a single phase of α-$NaFeO_2$ structure with the space group R3m. It is clear that both the 006/012 and the 108/110 are well resolved, indicating that all samples have a typical hexagonal layered structure. However, a small peak of impurity phase (Ni_2O_3) exists in this XRD pattern of sample annealed at 1,000 °C, which may be caused by the stronger Li volatilization loss at so high temperature.

The crystal parameters calculated from the XRD patterns based on the least-square method are shown in Table 1. As can be seen, both c and a increase with increasing the annealing temperature. Hence, the cell volume increases monotonously from 100.51 to 101.04 $Å^3$ with increasing annealing temperature from 800 to 1,000 °C. Nevertheless, the c/a value, which is an indicator of the degree of the hexagonal structure order, does not change with the annealing temperature. Besides, the

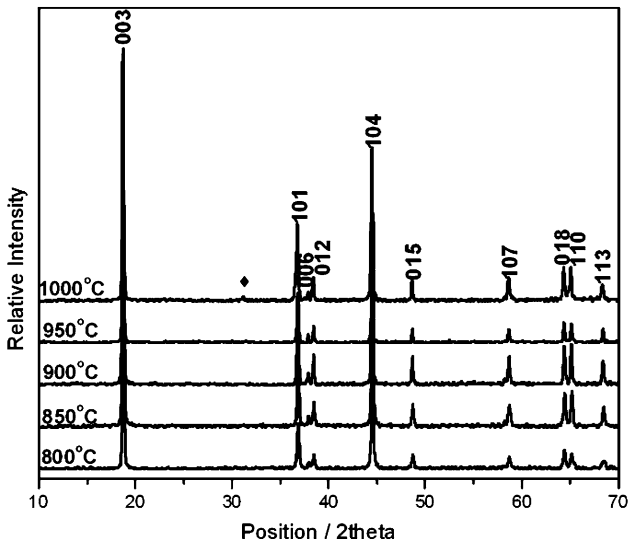

Fig. 1 XRD patterns of $LiCo_{1/3}Ni_{1/3}Mn_{1/3}O_2$ powders annealed at different temperatures (the annealing temperatures were indicated in the patterns).♦ sign represents Ni_2O_3 impurity

crystallite size calculated based on the (003) peak according to the Scherrer equation markedly grows with increasing the annealing temperature; they are 0.07, 0.1, 0.23, 0.32 and 0.34 μm for the annealing temperature of 800, 850, 900, 950 and 1,000 °C, respectively. This can be regarded as the enhancement of crystallinity of these powders.

To understand the above changes in the crystal structure, the lithium volatilization at a high annealing temperature should be taken into account. For the 5% Li-excessive starting composition, the prepared samples are more and more close to the stoichiometric $LiCo_{1/3}Ni_{1/3}Mn_{1/3}O_2$ as the lithium volatilization degree increases from 800 to 950 °C, which can be confirmed by literature work [16, 22]. Accordingly, the average valence of transition-metal ions in $Li_{1+x}Co_{1/3}Ni_{1/3}Mn_{1/3}O_2$ ($x \leq 0.05$) decreases with increasing the annealing temperature. Because the ionic radius of lower valence ions is bigger than that of higher valence, the cell parameters (a and c) and the unit-cell volume will display the increasing trend with increasing the annealing temperature.

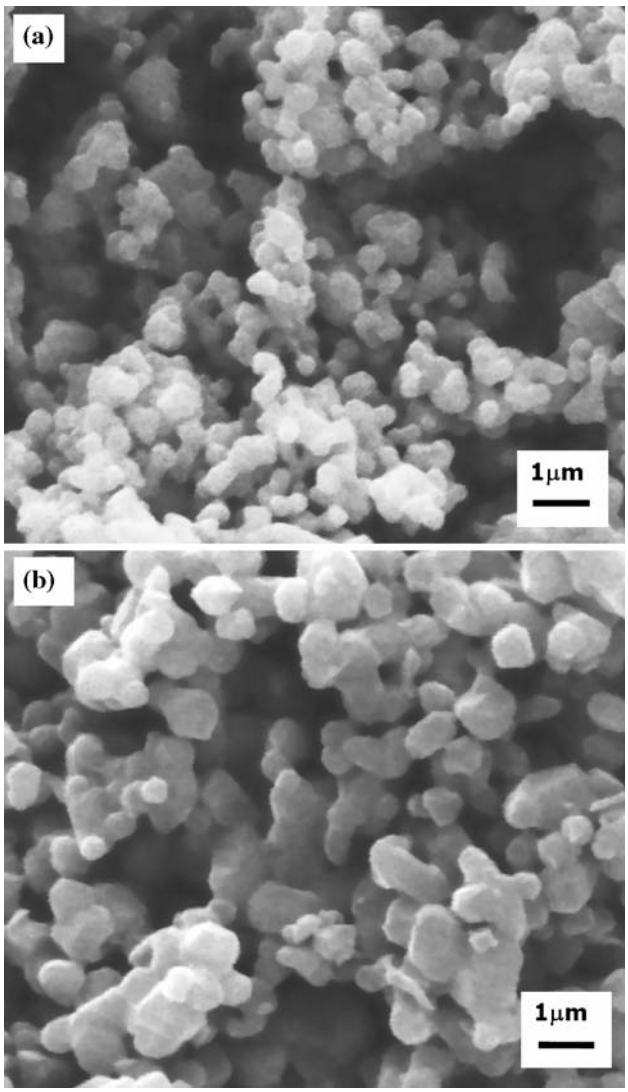

Fig. 2 SEM image of an as-prepared $LiCo_{1/3}Ni_{1/3}Mn_{1/3}O_2$ powder annealed at 900 °C (**a**) and 950 °C (**b**)

The scanning electron microscopy (SEM) images of the $LiCo_{1/3}Ni_{1/3}Mn_{1/3}O_2$ powders annealed at 900 and 950 °C are shown in Fig. 2. Obviously, the powders are composed of homogeneous round particles with an average particle size of around 0.3 μm after annealing at 900 °C and 1 μm

Table 1 Crystal parameters and coulombic efficiency of $LiCo_{1/3}Ni_{1/3}Mn_{1/3}O_2$ synthesized at different annealing temperatures (800–1,000 °C)

T (°C)	Lattice parameters				Calculated crystallite size (μm)	Battery performance
	c(Å)	a(Å)	c/a	Cell volume (Å^3)		First efficiency(%)
800	14.197(5)	2.859(1)	4.97	100.51	0.07	78.4
850	14.199(6)	2.859(1)	4.97	100.52	0.10	78.7
900	14.213(9)	2.861(2)	4.97	100.77	0.23	79.5
950	14.216(7)	2.860(9)	4.97	100.77	0.32	87.7
1000	14.222(6)	2.864(1)	4.97	101.04	0.34	75.7

after annealing at 950 °C. It is in agreement with the crystal growth theory and similar to the increasing trend of calculated crystallite size (Table 1). In addition, the powders annealed at the other temperatures have the same morphology (not shown here).

Electrochemical properties

Figure 3 shows the electrochemical performance of Li/$LiCo_{1/3}Ni_{1/3}Mn_{1/3}O_2$ cells in the voltage range between 2.8 and 4.5 V. It can be seen that for the $LiCo_{1/3}Ni_{1/3}Mn_{1/3}O_2$ powders annealed at different temperatures, the one annealed at 950 °C has the highest initial discharge capacity (178 mAh/g at C/6 rate), which is comparable to the discharge capacity (177 mAh/g at about C/9 rate) synthesized by hydroxide co-precipitation method with optimal conditions [17]. Its reversible long-cycling capacity is above 150 mAh/g at C/2 rate after 50 cycles. For comparison, the initial specific discharge capacities are 159, 164, 165 and 137 mAh/g for the samples annealed at temperatures of 800, 850, 900, and 1,000 °C. The initial specific discharge capacity gradually increases from 800 to 950 °C. Such a relationship between the electrochemical properties and the annealing temperature is mainly caused by following two factors. First, the crystallinity of a powder is one important factor affecting the electrochemical discharge capacity. Since the crystallinity of powder particles is enhanced with the increase of the annealing temperature (Table 1), the electrochemical capacity of electrode material is proportional to the crystallinity of powders annealed at temperatures from 800 to 950 °C. Second, the particle size of electrode material is also related to its electrochemical performance. Generally, a part of overall capacity is consumed to form a surface layer on the electrode particles during the first cycle. The smaller particle size means a greater specific surface area, resulting in higher capacity loss. As shown above, the particle size at 900 and 950 °C is around 0.3 and 1 μm, respectively (Fig. 2). This explains the result that the coulombic efficiency during the first cycle increases from 79.5 to 87.7% with varying the temperature from 900 to 950 °C (Table 1).

On the other hand, the electrode using the 1,000 °C-annealed $LiCo_{1/3}Ni_{1/3}Mn_{1/3}O_2$ shows the worst electrochemical properties in terms of capacity (Fig. 3) and coulombic efficiency (Table 1). This is likely related to the existence of the inactive impurity Ni_2O_3 in the powder (Fig. 1). Judging from all of the afore-mentioned evidences, we may reasonably conclude that the excellent electrochemical performance is related to the appropriate crystallinity, particle size and stoichiometry of an electrode powder. Therefore, for the RPG-derived $LiCo_{1/3}Ni_{1/3}Mn_{1/3}O_2$, the optimal annealing temperature can be safely considered at 950 °C.

Figure 4 illustrates the initial three charge and discharge curves of the 950 °C-annealed $LiCo_{1/3}Ni_{1/3}Mn_{1/3}O_2$ in the voltage range of 2.8–4.5 V. The current applied to the positive-electrode is C/6 rate. The charge capacity is 203 mAh/g and the irreversible capacity loss is about 12% in the first cycle. The irreversible capacity comes mainly from the fact that a part of Ni^{3+} cannot be reduced to Ni^{2+} after the first cycle [13]. Also, the formation of surface layer on the positive-electrode material is another main contributor to the irreversible capacity loss, especially for some materials of

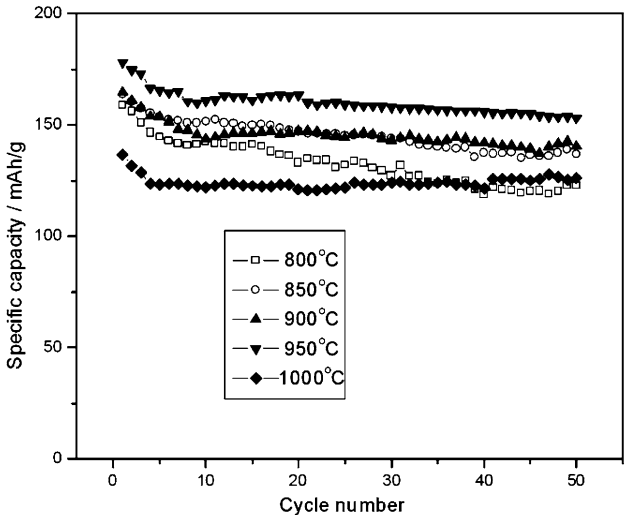

Fig. 3 Specific discharge capacity of $LiCo_{1/3}Ni_{1/3}Mn_{1/3}O_2$ positive-electrode materials as a function of cycle number. The current was C/6 for the initial three cycles and C/2 for the rest of cycles. The range of cell voltage is between 2.8 and 4.5 V

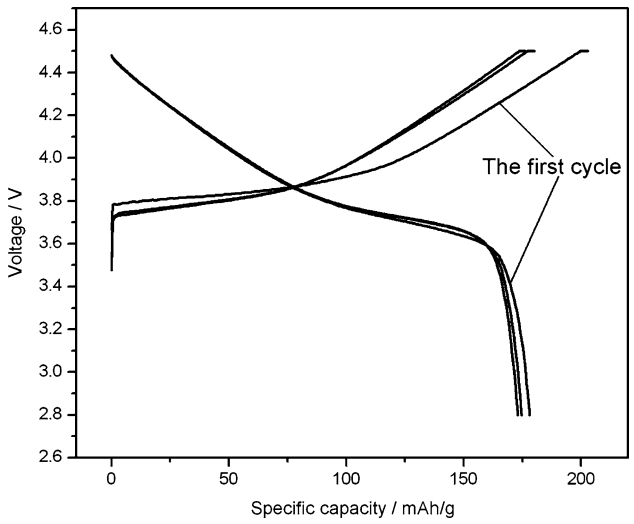

Fig. 4 The voltage profile of $Li(Ni_{1/3}Co_{1/3}Mn_{1/3})O_2$ (prepared at 950 °C) for initial three cycles in the voltage range of 2.8–4.5 V at a current of C/6

small particle sizes. For the 950 °C-annealed $LiCo_{1/3}Ni_{1/3}Mn_{1/3}O_2$, the coulombic efficiency is found to be higher than 99% after the first cycle, indicating that the activated electrode material is of stable crystal structure.

In order to investigate the rate capability of the positive-electrode material synthesized by RPG method, we measured the charge/discharge behaviors of the cell using 950 °C-annealed $LiCo_{1/3}Ni_{1/3}Mn_{1/3}O_2$ at different C-rates from 0.2 to 8C. The same C rate current was adopted in charge and discharge process, meaning that the fast-charge and fast-discharge mode was carried out to the cells. As can be seen from Fig. 5, the reversible capacities of the cell at 0.2, 0.4, 0.8, 1.5, 2.5, 4 and 8C are 173, 160, 154, 147, 137, 116 and 67 mAh/g, respectively. The data represent a rather good rate capability for this positive-electrode material.

Figure 6 shows the cyclic voltammogram (CV) of the cell using 950 °C-annealed $LiCo_{1/3}Ni_{1/3}Mn_{1/3}O_2$ as the positive-electrode material in the voltage range of 2.8–4.7 V vs. Li/Li^+. As observed, there are two couples of extraction/insertion peaks at around 3.7 V (strong) and 4.5 V (weak) in every charge/discharge cycle. Similar CV curves have been reported by other groups [23–26]. The sharp and intense peaks around 3.7 V are assigned to the process of Ni^{2+}/Ni^{4+} transition, but the weak coupled peaks around 4.5 V are in the state of argument. Chung et al. [23] think that the peaks around 4.5 V are related to Co^{3+}/Co^{4+} redox reactions. Recently, Manthiram et al. [24] found that they are closely related to the higher surface area of the positive-electrode material and it exhibits more pronounced in manganese-rich compositions compared to the nickel- and cobalt-rich compositions. In our case, the

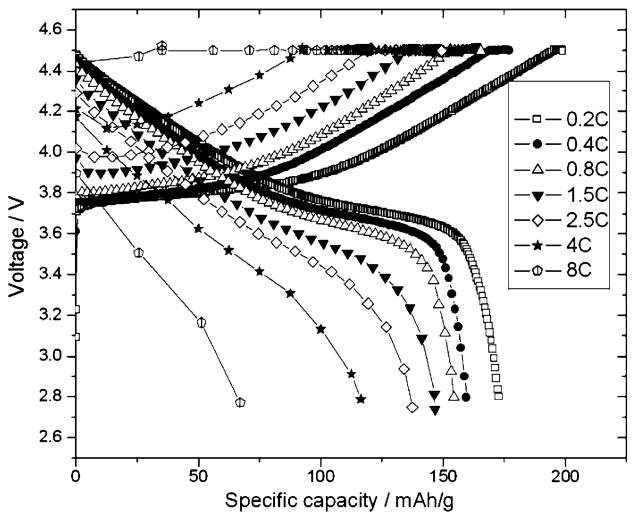

Fig. 5 Rate capability of a cell $Li/LiCo_{1/3}Ni_{1/3}Mn_{1/3}O_2$ using the sample annealed at 950 °C. The mode of fast charge and fast discharge is adopted. The cell was charged with a current of 0.2, 0.4, 0.8, 1.5, 2.5, 4, 8 to 4.5 V, then held at 4.5 V until the current dropped to less than the current of about C/20. The discharge current is 0.2, 0.4, 0.8, 1.5, 2.5, 4, 8C, respectively

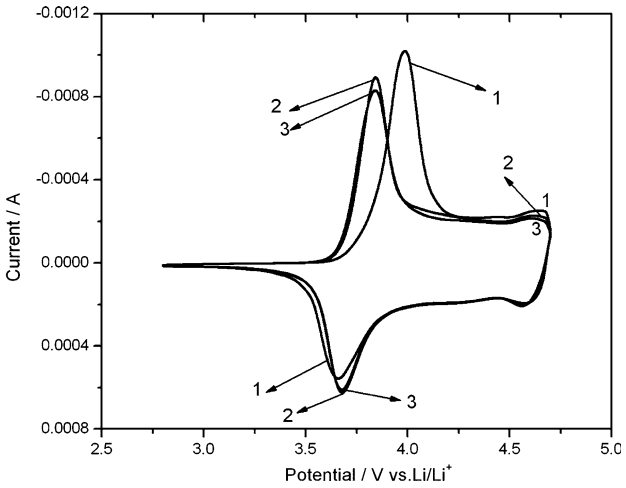

Fig. 6 Cyclic voltammogram (CV) of the $Li(Ni_{1/3}Co_{1/3}Mn_{1/3})O_2$ electrode using 950 °C-annealed $Li(Ni_{1/3}Co_{1/3}Mn_{1/3})O_2$ positive-electrode material in the range of 2.8–4.7 V vs. Li/Li^+

former scenario seems more reasonable according to following more evidences. Deb et al. [15] also found that the average valence of Co ions begins to increase when the cell voltage is around 4.5 V, but keeps as Co^{3+} before this point. Also, the Co^{3+}/Co^{4+} redox transition should occur in the range of $2/3 \leq x \leq 1$ in $Li_{1-x}(Ni_{1/3}Co_{1/3}Mn_{1/3})O_2$ according to the first principle calculation [6].

Conclusions

We successfully introduced γ-ray radiation to the process of preparing pure-phase $LiCo_{1/3}Ni_{1/3}Mn_{1/3}O_2$, with a simple method of Radiated polymer gel method (RPG). The cell parameters (a and c), unit-cell volume and crystallinity of the synthesized $LiCo_{1/3}Ni_{1/3}Mn_{1/3}O_2$, powders increase with increasing the annealing temperature between 800 and 1,000 °C. Electrochemical measurements indicate that the optimal annealing temperature is 950 °C. This 950 °C-annealed $LiCo_{1/3}Ni_{1/3}Mn_{1/3}O_2$ powder shows an initial discharge capacity of 178 mAh/g at C/6 rate. It has also rather good rate capability with the specific capacity of 173 mAh/g at 0.2C and 116 mAh/g at 4C.

Acknowledgements This study was supported by National Science Foundation of China (Grant Nos. 50372064 and 20471057). We are also grateful to the China Education Ministry (SRFDP No. 2003035057). The USTC radiation chemistry laboratory has provided the assistance for the experiments of γ-ray radiation.

References

1. Mizushima K, Jones PC, Wiseman PJ, Goodenough JB (1980) Mater Res Bull 15:783

2. Reimers JN, Dahn JR (1992) J Electrochem Soc 139:2091
3. MacNeil DD, Lu ZH, Dahn JR (2002) J Electrochem Soc 149:A1332
4. Shaju KM, Bruce PG (2006) Adv Mater 18:2330
5. Ohzuku T, Makimura Y (2001) Chem Lett 642
6. Koyama Y, Tanaka I, Adachi H, Makimura Y, Ohzuku T (2003) J Power Sources 119:644
7. Yabuuchi N, Ohzuku T (2003) J Power Sources 119–121:171
8. Yabuuchi N, Ohzuku T (2005) J Power Sources 146:636
9. Koyama Y, Yabuuchi N, Tanaka I, Adachi H, Ohzuku T (2004) J Electrochem Soc 151:A1545
10. Yabuuchi N, Koyama Y, Nakayama N, Ohzuku T (2005) J Electrochem Soc 152:A1434
11. Choi J, Manthiram A (2005) J Electrochem Soc 152:A1714
12. Hwang BJ, Tsai YW, Carlier D, Ceder G (2003) Chem Mater 15:3676
13. Tsai YW, Hwang BJ, Ceder G, Sheu HS, Liu DG, Lee JF (2005) Chem Mater 17:3191
14. Yoon W, Grey CP, Balasubramanian M, Yang X, Fisher DA, MacBreen J (2004) Electrochem Solid-State Lett 7:A53
15. Deb A, Bergmann U, Cramer SP, Cairns EJ (2005) J Appl Phys 97:113523
16. Cho TH, Park SM, Yoshio M, Hirai T, Hideshima Y (2005) J Power Sources 142:306
17. Lee MH, Kang YJ, Myung ST, Sun YK (2004) Electrochim Acta 50:939
18. Tong DG, Lai QY, Wei NN, Tang AD, Tang LX, Huang KL, Ji XY (2005) Mater Chem Phys 94:423
19. Li DC, Muta T, Zhang LQ, Yoshio M, Noguchi H (2004) J Power Sources 132:150
20. Ding N, Ge XW, Chen CH (2005) Mater Res Bull 40:1451
21. Xu HY, Xie S, Ding N, Liu BL, Shang Y, Chen CH (2006) Electrochim Acta 51:4352
22. Myung ST, Komaba S, Kurihara K, Hosoya K, Kumagai N, Sun YK, Nakai I, Yonemura M, Kamiyama T (2006) Chem Mater 18:1658
23. Kim JM, Chung HT (2004) Electrochim Acta 49:937
24. Choi J, Manthiram A (2005) Electrochem Solid-State Lett 8:C102
25. Shaju KM, Subba Rao GV, Chowdari BVR (2002) Electrochim Acta 48:145
26. Li DC, Muta T, Zhang LQ, Yoshio M, Noguchi H (2004) J Power Sources 132:150